

A single-scan protocol for absolute $D_{2/3}$ receptor quantification with [123 I] IBZM SPECT

Stergios Tsartsalis^{a,b,c}, Benjamin B. Tournier^a, Karl Aoun^a, Selim Habiby^a, Diego Pandolfo^a, Andrea Dimiziani^a, Nathalie Ginovart^{a,c}, Philippe Millet^{a,c,*}

^a Vulnerability Biomarkers Unit, Division of Adult Psychiatry, Department of Mental Health and Psychiatry, University Hospitals of Geneva, Switzerland

^b Division of Addictology, Department of Mental Health and Psychiatry, University Hospitals of Geneva, Switzerland

^c Department of Psychiatry, University of Geneva, Switzerland

ARTICLE INFO

Keywords:
[123 I]IBZM
SPECT
 $D_{2/3}$ receptor
Rat

ABSTRACT

Purpose: Molecular imaging of the $D_{2/3}$ receptor is widely used in neuropsychiatric research. Non-displaceable binding potential (BP_{ND}) is a very popular quantitative index, defined as the product of the receptor concentration (B_{avail}) and the radiotracer affinity for the receptor ($1/appK_d$). As the $appK_d$ is influenced by parameters such as the endogenous neurotransmitter dynamics, it often constitutes a confounding factor in research studies. A simplified method for absolute quantification of both these parameters would be of great interest in this context. Here, we describe the use of a partial saturation protocol that permits to produce an *in vivo* Scatchard plot and thus estimate B_{avail} and $appK_d$ separately, through a single dynamic SPECT session. To validate this approach, a multi-injection protocol is used for the full kinetic modeling of [123 I]IBZM using a 3-tissue compartment, 7-parameter model (3T-7k). Finally, more “classic” BP_{ND} estimation methods are also validated against the results of the 3T-7k.

Methods: Twenty-nine male rats were used. Binding parameters were estimated using the 3T-7k in a multi-injection protocol. A partial saturation protocol was applied at the region- and voxel-level and results were compared to those obtained with the 3T-7k model. The partial saturation protocol was applied after an adenovirus-mediated D_2 receptor striatal overexpression and in an amphetamine-induced dopamine release paradigm. The Simplified Reference Tissue Model (SRTM), the Logan's non-invasive graphical analysis (LNIGA) and a simple standardized uptake ratio (SUR) method were equally applied.

Results: The partial saturation experiments gave similar values as the 3T-7k both at the regional and voxel-level. After adenoviral-mediated D_2 -receptor overexpression, an increase in B_{avail} by approximately 18% was observed in the striatum. After amphetamine administration, a 16.93% decrease in B_{avail} ($p < 0.05$) and a 39.12% increase ($p < 0.01$) in $appK_d$ was observed. BP_{ND} derived from SRTM, LNIGA and SUR correlated well with the B_{avail} values from the 3T-7k ($r=0.84$, $r=0.84$ and $r=0.83$, respectively, $p < 0.0001$ for all correlations).

Conclusion: A partial saturation protocol permits the non-invasive and time-efficient estimation of B_{avail} and $appK_d$ separately. Given the different biological phenomena that underlie these parameters, this method may be applied for the in-depth study of the dopaminergic system in translational molecular imaging studies. It can detect the biological variations in these parameters, dissociating the variations in receptor density (B_{avail}) from affinity ($1/appK_d$), which reflects the interactions of the receptor with its endogenous ligand.

1. Introduction

Molecular imaging of the dopaminergic system has been a particularly useful tool in the study of neurobiological mechanisms of neuropsychiatric disorders. Single photon emission tomography (SPECT) with [123 I]IBZM permits the *in vivo* study of striatal $D_{2/3}$ receptors in human and translational studies with a particular interest

in psychosis and addiction (Abi-Dargham et al., 2009; Murnane and Howell, 2011). Molecular imaging enables a wide range of functional studies ranging from $D_{2/3}$ receptor quantification, receptor occupancy by medications to the effect of induced endogenous dopamine release across physiological and pathological conditions (Kugaya et al., 2000).

Full pharmacokinetic modeling requires a complex scanning protocol to identify the absolute neuroreceptor density, available for

* Correspondence to: Vulnerability Biomarkers Unit, Division of Adult Psychiatry, Department of Mental Health and Psychiatry, University Hospitals of Geneva, Switzerland, Chemin du Petit-Bel-Air 2, CH1225 Chêne-Bourg, Switzerland.

E-mail address: Philippe.Millet@hcuge.ch (P. Millet).

<http://dx.doi.org/10.1016/j.neuroimage.2016.12.050>

Received 12 September 2016; Accepted 18 December 2016

Available online 21 December 2016

1053-8119/ © 2016 Elsevier Inc. All rights reserved.

binding (B_{avail}) and the kinetic constants governing the transfer of the radiotracer between the plasma- and tissue compartments as well as its interaction with the receptor. Furthermore, it is highly invasive. Regarding the radiotracer-receptor interactions, the ratio of radiotracer dissociation (k_{off}) and association constants (k_{on}) provides the equilibrium dissociation constant ($\text{app}K_d$), which equals the inverse of radiotracer affinity ($1/\text{app}K_d$) (Delforge et al., 1989, 1990). Because of technical limitations inherent to the complexity of scanning protocols and the limited parameter identifiability, pharmacokinetic models are simplified with respect to the number of compartments and parameters to be estimated: thus, B_{avail} and $\text{app}K_d$ are jointly estimated as the binding potential ($\text{BP} = B_{\text{avail}}/\text{app}K_d$), perhaps the most popular index of receptor density in *in vivo* imaging studies (Innis et al., 2007). Beyond this simplification, the use of a brain region devoid of the receptor under study as an index of non-displaceable binding abolishes the need for arterial blood sampling and estimation of the model's input function (Gunn et al., 1997; Lammertsma and Hume, 1996; Logan et al., 1996). It is important to note that these simplified approaches may introduce significant bias in biological studies if not properly validated (Shrestha et al., 2012) against the “gold-standard” quantitative neuroreceptor estimates obtained with full pharmacokinetic modeling.

The use of BP as a quantitative measure in *in vivo* molecular neuroimaging may reflect the B_{avail} of the receptor under study only if the radiotracer's affinity for the receptor (thus the $\text{app}K_d$) remains stable across subjects of a given population in physiological conditions and disease states. However, there is evidence pointing to variations in a radiotracer's affinity for its target-receptor, violating this assumption. For instance, a radiotracer and the endogenous ligand (e.g. the neurotransmitter) present a competitive binding to the receptor. Baseline neurotransmitter levels in the vicinity of the receptor as well as challenge-induced neurotransmitter changes both vary with respect to physiological parameters and pathological conditions (Kuwabara et al., 2012; Narendran and Martinez, 2008; Vaessen et al., 2015; Volkow et al., 2009a), thereby modifying $\text{app}K_d$ while changes in B_{avail} may also occur in the same contexts. Using BP over-simplifies the study of such complex phenomena. In other words, a simplified method of *in vivo* estimation of B_{avail} and $\text{app}K_d$ would be of utmost value, particularly in studies of dopamine neurochemistry.

The *in vivo* separate estimation of B_{avail} and $\text{app}K_d$ has been described by Delforge et al. (1996, 1997, 1993); Vivash et al. (2014) for the quantification of benzodiazepine receptors in the human brain using [^{11}C]flumazenil positron emission tomography (PET). In this approach, a quantity of unlabeled radiotracer compound is co-injected with the labeled radiotracer to induce a partial saturation of the receptor sites. The pharmacological properties of the radiotracer permit the equilibrium to be rapidly installed. Delforge et al. proposed

the saturation of at least 50% of receptor sites in order to permit a rapid decrease in specific binding during the scan duration. Plotting the ratio of specific to non-displaceable binding against specific binding forms a Scatchard plot from which B_{avail} and $\text{app}K_d$ can be deduced. Ideally, receptor occupancy should not exceed 70% so that a relatively large number of points are aligned within the regression line. A region devoid of receptor gives an estimate of the non-displaceable binding, further simplifying the quantification.

In this study, we describe a partial saturation approach for the *in vivo* estimation of B_{avail} and $\text{app}K_d$ with [^{123}I]IBZM SPECT using a single-scan protocol in the region- and voxel-level. This method is validated against the results of full pharmacokinetic modeling with a multiple-injection protocol that provides the “gold-standard” estimates of all kinetic parameters along with B_{avail} and $\text{app}K_d$. Other simplified methods to estimate BP without input function estimation are validated against the aforementioned results.

2. Materials and methods

2.1. Animals and general SPECT scan protocol

Thirty-two male Sprague-Dawley rats (Janvier Laboratories, Le Genet-St-Isle, France), weighing between 380 and 500 g were employed in the study. Of these, three rats were employed in an *in vivo* multi-injection SPECT imaging protocol for absolute $D_{2/3}$ receptor quantification. One rat was employed in a long (180 min) single-injection SPECT scan. Four rats were employed in an arterial plasma analysis for the study of plasma kinetics of the radiotracer and the estimation of the free parent radiotracer fraction. Fourteen rats were employed in an *ex vivo* study to determine the dose-occupancy relationship of the unlabeled IBZM when co-injected with the radiolabeled compound (described in Supplementary Materials and Methods S1.2). Two rats were employed in a presaturation SPECT study (described in detail in Supplementary Materials and Methods S1.3). Seven rats were employed in a SPECT experiment with a partial $D_{2/3}$ receptor saturation design for the determination of B_{avail} and $\text{app}K_d$ parameters from an *in vivo* Scatchard plot. Two rats out of seven of the partial saturation experiment were employed in an *in vivo* study of the effect of amphetamine-induced dopamine release on the B_{avail} and $\text{app}K_d$ parameters as determined with two SPECT scans with a partial saturation design, one before and one after amphetamine administration. Finally, one rat was employed in an adenoviral-mediated D_2 -receptor overexpression experiment. The repartition of rats is summarized in Table 1.

SPECT scans were performed with a U-SPECT-II camera (MiLabs, Utrecht, Netherlands). In rats that underwent SPECT scans with the multi-injection protocol, two polyethylene catheters (i.d.=0.58 mm,

Table 1
Repartition of rats into experimental groups.

Experiment	n	Methods	Model/Outcome measures
Multi-injection protocol	3	SPECT scan and arterial blood sampling	3T-7k/ B_{avail} , $\text{app}K_d$, K_1 , k_2 -6 SRTM, LNIGA, SUR/BP _{ND} SRTM, Full RTM, 2-TRM
Single-injection protocol	1	SPECT scan of a long duration (180 min)	Tri-exponential model of free parent radiotracer in arterial plasma
Free parent radiotracer fraction estimation	4	Serial arterial blood sampling after radiotracer injection and TLC	Receptor occupancy
Dose- occupancy curve for unlabeled IBZM	14	<i>Ex-vivo</i> whole-tissue radioactivity measurements after administration of various doses of unlabeled IBZM along with labeled radiotracer	
Presaturation study	2	A 50-min long SPECT scan after administration of fully-saturating doses of unlabeled IBZM	Relationship between the non-displaceable binding in striatum and cerebellum (r factor)
<i>In vivo</i> Scatchard analysis study	5	SPECT scan after co-injection of a partially saturating dose of unlabeled compound, along with labeled one	Scatchard plot analysis/ B_{avail} , $\text{app}K_d$
	1	SPECT scan as above after AAV-mediated overexpression of D_2 receptors in unilateral striatum	
	2	Two SPECT scans as above, the second preceded by administration of amphetamine (15 mg/kg, i.v.)	

$\text{o.d.} = 0.96 \text{ mm}$) were inserted in the left femoral vein and artery for radiotracer administration and blood sampling, respectively. SPECT scans were performed under isoflurane anesthesia (3% for induction and 1–2% for maintenance). In rats that underwent SPECT scans for the partial saturation protocol or *ex vivo* imaging, radiotracer injection was performed via a tail vein catheter. Body temperature was monitored during the scans and maintained at $37 \pm 1^\circ\text{C}$ by means of a thermostatically controlled heating blanket.

SPECT image reconstruction was performed using a pixel ordered subsets expectation maximization (P-OSEM, 0.4-mm voxel size, 4 iterations, 6 subsets) algorithm using MiLabs image reconstruction software. Radioactive decay correction was performed while correction for attenuation or scatter was not. Following reconstruction, dynamic images from the partial saturation experiment were denoised with factor analysis (FA) using Pixies software (Apteryx, Issy-les-Moulineaux, France) as previously described (Tsartsalis et al., 2014). FA permits the decomposition of dynamic signal into a few elementary components, termed factors (Di Paola et al., 1982; Millet et al., 2012; Tsartsalis et al., 2014). In this study, four factors were retained and the rest of the signal was discarded as noise.

All experimental procedures were approved by the Ethical Committee on Animal Experimentation of the Canton of Geneva, Switzerland.

2.2. Radiotracer preparation

^{123}I radioiodide was purchased from Heider AG (Schöftland, Switzerland). ^{123}I IBZM was obtained by incubation, for 15 min at 68°C , of a mixture containing 5 μl of BZM precursor (24 nmol/ μl in ethanol), 2 μl of glacial acetic acid, 1 μl of 30% H_2O_2 and 10 mCi of carrier-free ^{123}I sodium iodide in 0.05 M NaOH. Radiotracer was isolated by a linear gradient HPLC run (from 5% acetonitrile, ACN, to 95% ACN, 10 mM H_3PO_4 , in 10 min).

HPLC was equipped with a reverse-phase column (Phenomenex Bonclone C18, Phenomenex, Schlieren, Switzerland) and radiotracer was eluted at a flow of 3 ml/min. Fractions containing ^{123}I IBZM were diluted in water and loaded on a Sep-Pak cartridge (Sep-Pak C18, Waters, Switzerland). ^{123}I IBZM was eluted with 0.5 ml of 95% ACN, 10 mM H_3PO_4 and concentrated using a rotary evaporator, and the final product was diluted in saline prior to animal administration.

2.3. SPECT single- and multi-injection imaging and quantification, arterial plasma analysis and free parent radiotracer fraction estimation

A multi-injection protocol for full kinetic modeling of ^{123}I IBZM was employed (Millet et al., 2006; Millet et al., 2012). The scan protocol began with a first injection of the radiotracer ($91.47 \pm 2.91 \text{ MBq}$) at a high specific activity ($934.04 \pm 114.37 \text{ GBq}/\mu\text{mol}$), followed by a second co-injection of ^{123}I IBZM ($93.06 \pm 7.11 \text{ MBq}$) and the unlabeled compound (6.2 nmol/kg) at 120 min and a third injection of the unlabeled compound only at 180 min (1.24 $\mu\text{mol}/\text{kg}$). The overall scan protocol included 240 1-minute frames.

During dynamic SPECT acquisitions, forty arterial blood samples (of 25 μl each) were withdrawn after each radiotracer injection at regular time intervals. Radioactivity was measured in a gamma counting system and expressed in kBq/ml after calibration. To estimate the plasma input function in *in vivo* SPECT experiments, only whole-blood radioactivity was measured individually.

Metabolite correction and plasma protein binding analysis for the estimation of radiotracer plasma input function was performed in an independent group of four rats, as previously described (Gandelman et al., 1994; Millet et al., 2008, 2012; Mintun et al., 1984; Tsartsalis et al., 2014, 2015). A detailed description can be found in [Supplementary Materials and Methods paragraph S1.1](#).

To evaluate the pharmacokinetic behavior of ^{123}I IBZM in scans

with a longer duration, a 180-min scan was performed using one rat. The scan protocol began with an injection of the radiotracer (66.6 MBq) at a high specific activity ($> 900 \text{ GBq}/\mu\text{mol}$). The overall scan protocol included 80 2-minute frames.

2.4. In vivo Scatchard plot study

A partial saturation imaging experiment was designed to estimate B_{avail} and appK_d as proposed by Delforge et al. (1996, 1997) and optimized by Wimberley et al. (2014a, b). In theory, the original Scatchard plot can be approached with an *in vivo* imaging experiment by plotting the specifically bound fraction of radiotracer activity in a given region (C_s) versus the ratio of specific-to-non-displaceable binding in the same region (C_s/C_{ND}) during the time course of a single imaging experiment. When a dose of unlabeled compound is co-administered with the radiotracer at a concentration to occupy 50–70% of the receptor binding sites, the natural decrease of radiotracer binding over time permits to the different points of the plot to form a straight line when equilibrium has been reached. B_{avail} and appK_d may be estimated from the intercept to the C_s axis and the inverse of the line slope, respectively.

SPECT scans and image reconstruction were performed in the same conditions as in experiment 2.3. A single radiotracer injection ($50.8 \pm 6.3 \text{ MBq}$) (containing a dose of unlabeled IBZM determined in the *ex vivo* occupancy study, described in [supplementary Materials and Methods section S1.2](#) and leading to specific activities of $8.94 \pm 0.33 \text{ GBq}/\mu\text{mol}$) was followed by a scan composed of 90 frames of 1-min. No arterial blood sampling took place and cerebellum was employed as the reference region.

2.5. Simulation study, adenovirus-mediated D_2 receptor overexpression and amphetamine-induced dopamine release experiment

A simulation study was also performed to verify the validity of the Scatchard equilibrium conditions across different B_{avail} and appK_d parameters values: using the results of one multi-injection experiment, we simulated striatal specific- and free-binding TACs corresponding to a 30% higher and lower B_{avail} and appK_d using a partially saturating dose of unlabeled IBZM compound (see results section).

One animal was employed in the D_2 -receptor overexpression experiment by a stereotactic viral injection. The $D_2\text{R}$ adenovirus was generated using the pENTR directional TOPO cloning kit (Invitrogen) and the pAD/CMV/V5-DEST gateway vectors kit (Invitrogen). Briefly, the full-length cDNA corresponding to the sequence of *rattus* $D_2\text{R}$ was inserted into the pENTR vector. After plasmid purification from transformed Top10 competent cells, the cDNA was transferred into the pAD/CMV/V5-DEST vector by means of the Gateway system using LR Clonase. Following propagation of plasmids in Top10 competent cells, the recombinant adenoviral DNA was digested with PacI (New England Biolabs) and purified (QIAquick nucleotide removal kit, Qiagen). Linear $D_2\text{R}$ adenovirus was transfected into subconfluent 293 A cells according to the manufacturer's instructions (ViraPower Adenovirus Expression System, Invitrogen). The 293 A cells were cultured until regions of cytopathic effect are clearly observed (1–2 weeks). Cells and culture medium were centrifuge and freeze-thawed twice (-80°C overnight; $+25^\circ\text{C}$, 15 min) to obtain the adenovirus-enriched supernatants. Aliquots of the crude viral stock were used to amplify $D_2\text{R}$ adenovirus using fresh 293 A cell cultures. After amplification, $D_2\text{R}$ adenovirus were purified using the Vivapure AdenoPack 500 kit (Sartorius) and titered using the QuickTiter Adenovirus Titer Immunoassay Kit (Cell Biolabs). The $D_2\text{R}$ adenovirus titer was of 2×10^{10} infectious units per ml (Ifu/ml).

The animal was anesthetized with 2.5% isoflurane in O_2 and preventively treated against postoperative pain with buprenorphine (0.05 mg/kg, s.c.). Gel moisturizer (Lacryvisc) was applied on both eyes

and a 2 mm diameter hole was carefully drilled through the skull at the injection site. Two microliters of the D₂R adenovirus were injected in the left striatum (coordinates from bregma: anteroposterior = −0.5 mm; lateral = +3.0 mm; dorsoventral = −5.0 mm).

In two out of six rats of the partial saturation experiment of paragraph 2.5, a second partial saturation experiment (under the exact same conditions) took place two days after the first SPECT scan, preceded by an amphetamine injection (1.5 mg/kg i.v.) at 30 min before the radiotracer injection. This preliminary study aimed to evaluate the efficacy of this partial saturation paradigm to detect changes on the B_{avail} and $\text{app}K_d$ parameters owed to the amphetamine-induced dopamine release in the striatum.

2.6. Data analysis

SPECT images were processed with PMOD software v3.7 (PMOD Technologies Ltd, Zurich, Switzerland). Averaged images corresponding to the first ten frames of acquisition were co-registered to an MRI template integrated in PMOD (Schiffer et al., 2006). Transformation matrices were then applied to dynamic images. Tissue-activity curves (TACs) from the striatum as a whole, from the striatal sub-regions (Caudate-Putamen, CP, and Nucleus Accumbens, NAcc, bilaterally), and cerebellum were extracted from dynamic images using the predefined VOI template integrated in PMOD.

Several model configurations were employed for quantitative analysis of radiotracer kinetics in the multi-injection experiments. The whole multi-injection study TAC data was fitted with a two-tissue compartment five-parameter model (2T-5k), to estimate K_1 , k_2 , k_{on} , k_{off} and B_{avail} and a three-tissue compartment seven-parameter model (3T-7k) in order to obtain K_1 , k_2 , k_{on} , k_{off} , k_5 , k_6 and B_{avail} and the binding potential ($\text{BP} = B_{\text{avail}}/\text{app}K_d$). Given the number of parameters to estimate with the 3T-7k model and the subsequent low identifiability of model parameters, k_{off} was fixed at a pre-determined value after a preliminary fit of the model on whole-striatum TACs from the three rats, as previously described (Ginovart et al., 2001; Millet et al., 1995, 2006, 2000b). Average k_{off} value was fixed for further application of 3T-7k. The free, non-metabolized radiotracer fraction in the plasma was used as the input function (Delforge et al., 1999). Analysis was performed in Matlab software R2015b (Mathworks, USA). All other models were applied using PMOD software. TAC data corresponding to the first (high specific activity) injection of the multi-injection experiments were fitted with the 1) Simplified reference tissue model (SRTM) and the 2) Logan non-invasive graphical analysis (hereon, LNIGA), using a pre-defined k_2' value estimated with the SRTM, to obtain BP_{ND} images (Innis et al., 2007). Cerebellum was used as the reference region, given that no [¹²³I]IBZM specific binding is observed. Finally, the standardized uptake ratio (SUR) was obtained by normalizing delayed activity images to the activity in the reference region. For all methods of quantification, analysis was performed on TACs from the whole-striatum VOI as well as from the four sub-regions.

For SRTM and LNIGA, we evaluated the minimum duration of scan required to obtain stable binding parameters. BP_{ND} was estimated in whole-striatum TACs of diminishing duration (by 10-min decrements). The mean deviation of the BP_{ND} value, across the three rats, for a given scan duration from the value corresponding to the maximal duration was used as the evaluation criterion. A mean estimation within 5% of the parameter value at maximum duration with a coefficient of variation (CV) < 10% was considered a stable estimate. For SUR, BP_{ND} values were estimated over different fragments of data with a fixed-duration (10 min).

TACs from the long-duration single-injection study were first fitted with SRTM. To explain a misfit in the last time-points (see Results section), the full reference tissue model (Full-RTM) (Lammertsma et al., 1996) and the 2-tissue reference model (2-TRM) (Millet et al., 2002; Watabe et al., 2000) were also employed in PKIN. 2-TRM considers a second compartment in the reference region, correspond-

ing either to specific or non-specific binding. Kinetic constants corresponding to this compartment were fixed with average values extracted from the multi-injection study.

TACs from the partial saturation experiments (whole- and sub-regional striatal VOIs) were processed in a Matlab R2015b code. Data corresponding to the linear part of the Scatchard plot were used for the estimation of B_{avail} and $\text{app}K_d$ as previously described (Delforge et al., 1996). Cerebellum TAC was employed as an index of the non-displaceable binding in striatum. As described in [Supplementary Materials and Methods section S1.3](#), the ratio (r) of striatal-to-cerebellar non-displaceable binding was used to correct the cerebellar TAC (C_{cer}) before it was used in the Scatchard plot analysis, so $C_{\text{ND}} = r \times C_{\text{cer}}$ (Wimberley et al., 2014b). In addition, the Matlab R2015b code was employed to estimate B_{avail} and $\text{app}K_d$ at the voxel level in the striatum, after masking the extrastriatal voxels, using the TAC from the cerebellum as the non-displaceable binding index as in the VOI-level estimation. To evaluate the validity of voxel-wise application of the *in vivo* Scatchard analysis, we averaged the B_{avail} and $\text{app}K_d$ values in the striatum of each rat and compared it to the VOI-wise estimated value.

2.7. Statistical analysis

B_{avail} , $\text{app}K_d$ and BP_{ND} values resulting from fitting the data of the whole duration of the multi-injection protocol were used as the “gold standard” for comparison of estimations with the non-invasive quantification approaches by means of regression analysis. Comparisons of average B_{avail} and $\text{app}K_d$ values from the multi-injection study and the partial saturation experiments were performed by means of a two-samples t-test.

3. Results

3.1. Arterial plasma input function estimation

The mean percentage of non-metabolized radiotracer in the plasma was fitted with a triexponential function resulting in the following values: $A_1 = 0.035$, $B_1 = 0.0064$, $A_2 = 0.1097$, $B_2 = 0.3597$, $A_3 = 0.8546$, $B_3 = 42$. Average percentage of radiotracer bound to plasma proteins was 87.3%.

3.2. Full kinetic modeling of [¹²³I]IBZM with the multi-injection approach

Fit of the 3T-7k models is shown in [Fig. 1](#). 3T-7k provides excellent fits, while 2T-5k failed to fit, especially in cerebellar TACs: this is due to a non-negligible amount of non-specific binding, requiring the inclusion of the k_5 and k_6 parameters in the model that are the constants of radiotracer exchange between the free ligand and non-specific binding compartments. We thus only consider the results of 3T-7k fits for further comparisons in our study. Average B_{avail} values (in pmol/ml) were 13.41 ± 2.35 in left and 15.30 ± 1.35 in right NAcc. In the respective CP regions values were 20.28 ± 4.75 and 19.96 ± 1.87 . $\text{app}K_d$ values (in pmol/ml) were 6.21 ± 0.48 in left NAcc and 5.44 ± 0.45 in right NAcc. In CP, values were 7.20 ± 2.00 and 7.63 ± 2.87 , respectively.

Cerebellar TACs from the multi-injection protocol showed no radiotracer displacement with the third injection (unlabeled IBZM). The ratio of non-displaceable binding between the striatum and cerebellum was found equal to $r = 1.55 \pm 0.08$ ([Supplementary Materials and Methods S1.3 and Results S2.1](#)). Regarding the non-specific binding, given by the ratio of k_5/k_6 kinetic constants, it took values of 0.56 ± 0.21 in the whole-striatum VOI and 1.83 ± 0.50 in the cerebellum. The respective kinetic parameter values estimates in the individual sub-regions of the striatum are presented in [Table 2](#).

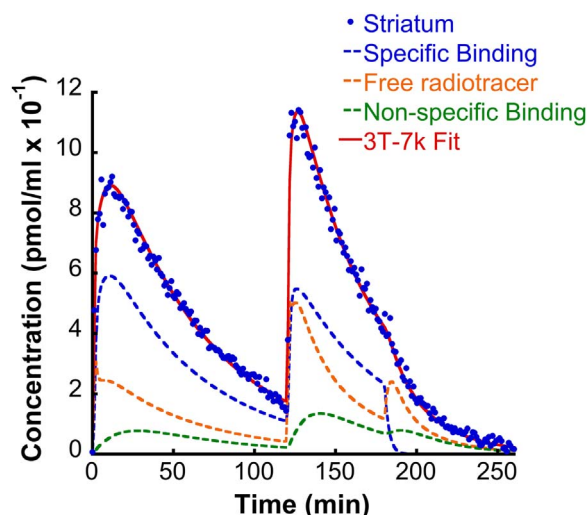


Fig. 1. TACs extracted from the striatum of one multi-injection dynamic SPECT scan, along with 3T-7k model fit and the kinetics specific, free and non-specific binding. Note the remnant striatal radioactivity at the end of the scan and after a displacement with unlabeled IBZM, explained the presence of non-specific binding.

3.3. BP_{ND} estimation using non-invasive approaches

SRTM and LNIGA, using cerebellum as reference region, provided excellent fits to data corresponding to the first injection (120 min) of the multi-injection scanning protocol. Average BP_{ND} values across the three rats are presented in Table 3. Application of both these models on TACs of diminishing duration revealed BP_{ND} values within 5% of the value at 120 min with a SD of < 10% for duration up to 70 min. Average striatal SUR values obtained from time fragments within the time window between 80 and 110 min of acquisition satisfied this stability criterion, thus, SUR values were estimated over data between the 80th and the 110th minute of acquisition for further comparisons in our study. Comparison of the quantitative estimates from all three non-invasive methods gave excellent correlations with B_{avail} values of the multi-injection protocol data ($r=0.84$ for SRTM, $r=0.84$ for LNIGA and $r=0.83$ for SUR, $p < 0.0001$ for all correlations) (Fig. 2).

The application of SRTM on TACs with a long duration (> 120 min) failed to provide an optimal fit (Fig. 3) as did the Full RTM. In contrast, only the 2-TRM provided an excellent fit to the whole range of data.

3.4. Partial saturation experiments

An injected dose between 12 and 24 nmol/kg occupies 50–70% of the receptors in the striatum as demonstrated in the *ex vivo* dose-occupancy study in 14 rats (see supplementary section S1.2 and supplementary Figure S1). 12 nmol/kg was the concentration of unlabeled compound that was co-injected with the radiotracer for the partial saturation scans.

Fig. 4a shows representative TACs obtained from the striatum and the cerebellum of a partial saturation experiment on one rat. The corresponding Scatchard plot is shown in Fig. 4b. The time-points that

Table 3

Mean and standard deviations of binding parameter estimates obtained from 3 rats.

VOI	$BP_{ND-SRTM}$	$\pm SD$	$BP_{ND-LNIGA}$	$\pm SD$	SUR	$\pm SD$
Acb L	1.52	0.16	1.53	0.15	3.46	0.76
Acb R	1.39	0.20	1.39	0.19	3.17	0.34
CP L	2.63	0.28	2.61	0.29	6.04	0.89
CP R	2.58	0.24	2.57	0.26	5.83	0.58

Acb: nucleus accumbens, CP: caudate-putamen, BP_{ND} values are unitless

were employed for the Scatchard analysis, for all rats were found between then 10th and the 45th minute post radiotracer injection. They provided a sufficiently high number of points to be used for tracing the regression line. Average B_{avail} values (pmol/ml) were 11.99 ± 8.47 in left and 16.36 ± 7.89 in right NAcc. In the respective CP regions values were 30.44 ± 7.57 and 28.77 ± 7.49 . $appK_d$ values (pmol/ml) were 8.38 ± 4.18 in left NAcc and 9.84 ± 3.16 in right NAcc. In CP, values were 10.57 ± 1.63 and 9.67 ± 1.60 , respectively (Table 4). B_{avail} and $appK_d$ values from the partial saturation experiment were in accordance with the respective values from the multi-injection study ($p > 0.05$ in two-sample t test). Fig. 5 shows a parametric image of B_{avail} , as estimated at the voxel level. Averaged voxel values correlated with VOI-wise estimates in an excellent manner ($r=0.96$, $p < 0.0001$).

3.5. Simulation study and application of the partial saturation protocol in adenoviral-mediated D_2 -receptor increase and amphetamine-induced dopamine release

The results of the simulation study are shown in Fig. 6a. Both a 30% increase and decrease in B_{avail} and $appK_d$ did not alter the validity of the Scatchard equilibrium conditions thereby permitting the extraction of unbiased parameter values from the Scatchard plot. The results of the partial saturation study in the rat that participated in the adenovirus-mediated D_2 -receptor overexpression experiment are shown in Fig. 6b. The ipsilateral striatum has a B_{avail} of 19.56 pmol/ml versus 16.58 pmol/ml in the contralateral striatum (an increase of 18%). $appK_d$ values were 5.40 pmol/ml and 5.56 pmol/ml, respectively. Finally, a coronal section of the parametric B_{avail} image of this rat is shown in Fig. 6c. In two of the six rats that were employed in the partial saturation study, a second SPECT scan under the same conditions was performed two days after the first one. Amphetamine (0.15 mg/kg) pretreatment led to an average 16.93% decrease in B_{avail} ($p < 0.05$ in a paired t-test comparison) and a 39.12% increase in $appK_d$ ($p < 0.01$), as shown in Figs. 7a and 7b, respectively.

4. Discussion

4.1. Full quantitative modeling of [123 I]IBZM and validation of non-invasive approaches

The present study presents and validates a wide range of applications of molecular imaging of the $D_{2/3}$ receptor in fundamental and – potentially- clinical research. To the best of our knowledge, this is the first description of full pharmacokinetic modeling of [123 I]IBZM in

Table 2

Mean and standard deviations of binding parameter estimates Obtained from 3 rats.

VOI	B_{avail}	$\pm SD$	$appK_d$	$\pm SD$	K_1	$\pm SD$	k_2	$\pm SD$	k_{on}	$\pm SD$	k_{off}	$\pm SD$	k_5	$\pm SD$	k_6	$\pm SD$
Acb L	13.41	2.35	6.21	0.48	1.09	0.32	0.09	0.02	0.06	0.005	0.4	–	0.04	0.02	0.04	0.02
Acb R	15.30	1.35	5.44	0.45	1.00	0.31	0.10	0.03	0.07	0.01	0.4	–	0.04	0.03	0.04	0.02
CP L	20.28	4.75	7.20	2.00	1.20	0.34	0.06	0.01	0.06	0.01	0.4	–	0.013	0.01	0.07	0.04
CP R	19.96	1.87	7.63	2.87	1.21	0.35	0.06	0.02	0.06	0.02	0.4	–	0.02	0.02	0.10	0.04
Cer	–	–	–	–	1.06	0.29	0.23	0.03	0.06	0.03	0.4	–	0.02	0.01	0.01	0.00

Acb: nucleus accumbens, CP: caudate-putamen, Cer: cerebellum, B_{avail} and $appK_d$ are in pmol/ml, K_1 in $mL \cdot cm^{-3} \cdot min^{-1}$, k_2 , k_3 , k_{off} , k_5 and k_6 in min^{-1}

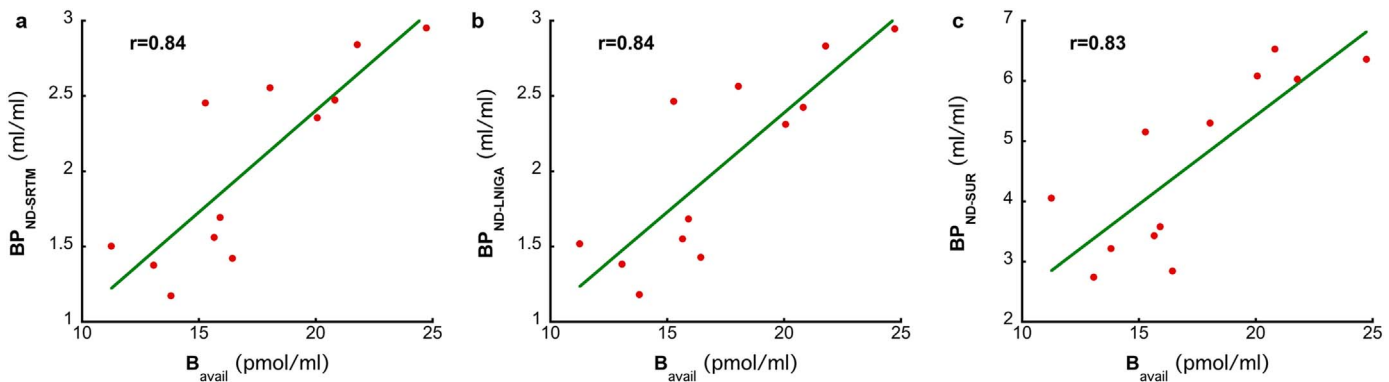


Fig. 2. Linear regression plots of comparisons between B_{avail} and BP_{ND} estimated with (a) SRTM, (b) LNIGA and (c) SUR.

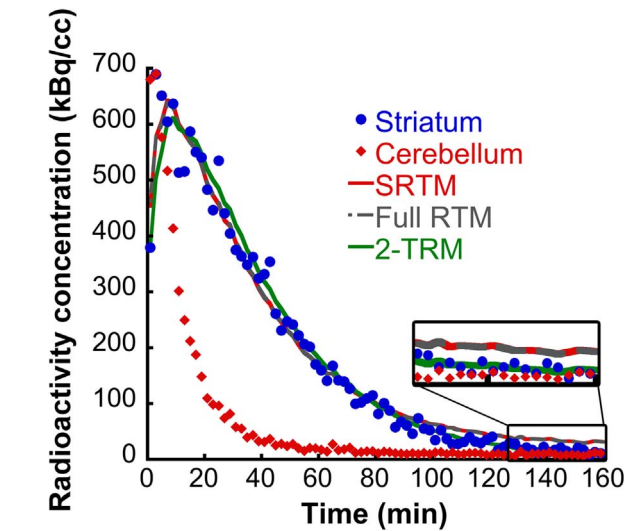


Fig. 3. TACs extracted from the striatum and cerebellum of data from the 180-min long single injection study. SRTM, Full-RTM and 2-TRM fits to the striatum. Note that SRTM and Full-RTM produce a misfit, especially during the latest time-points. 2-TRM fits well to the whole duration of data. In the magnified field, note the fits of the different models in detail.

in vivo. B_{avail} values in Caudate-Putamen and Nucleus accumbens are in accordance with values previously described by our group [Millet et al. \(2012\)](#) and others ([Mauger et al., 2005](#); [Wimberley et al., 2014b](#)), despite an apparent underestimation, probably due to a different

Table 4

Mean and standard deviations of B_{avail} and $appK_d$ estimates obtained from the partial saturation protocol in 7 rats.

VOI	B_{avail}	$\pm SD$	$appK_d$	$\pm SD$
Acb L	11.99	8.47	8.38	4.18
Acb R	16.37	7.89	9.85	3.17
CP L	30.44	7.57	10.58	1.64
CP R	28.77	7.49	9.67	1.61

Acb: nucleus accumbens, CP: caudate-putamen, B_{avail} and $appK_d$ are in pmol/ml

delineation of VOIs in the two studies. $appK_d$ values of this size range correspond to the modest affinity of [^{123}I]IBZM and are comparable for respective estimations for [^{11}C]raclopride in small animals ([Mauger et al., 2005](#); [Wimberley et al., 2014b](#)). As expected, no displaceable binding was observed in regions other than the striatum. The cerebellum was an exception, given that radioactivity binding in this “reference” region is used as an estimate of non-displaceable binding in striatum.

The multi-injection approach can be considered a “gold-standard” in modeling radiotracer kinetics in the brain, permitting an in-depth decomposition of the radioactive signal and full quantification of kinetic parameters, to our knowledge more than any other approach. Its use to validate simpler quantitative methods is invaluable ([Dumas et al., 2015](#); [Millet et al., 2002, 2000a, 2006, 2012](#)). However, the estimation of a high number of parameters through a very complex protocol naturally comes at a cost. Indeed, the full quantification of the kinetic parameters may sometimes be difficult and some assumptions

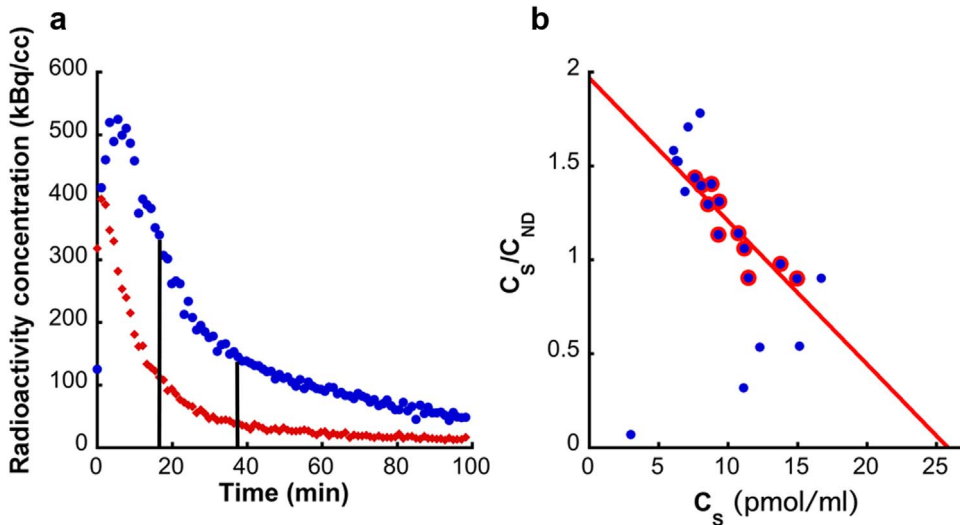


Fig. 4. (a) TACs extracted from the striatum and cerebellum of a partial saturation dynamic SPECT scan in one rat. (b) Corresponding Scatchard plots along with linear fit.

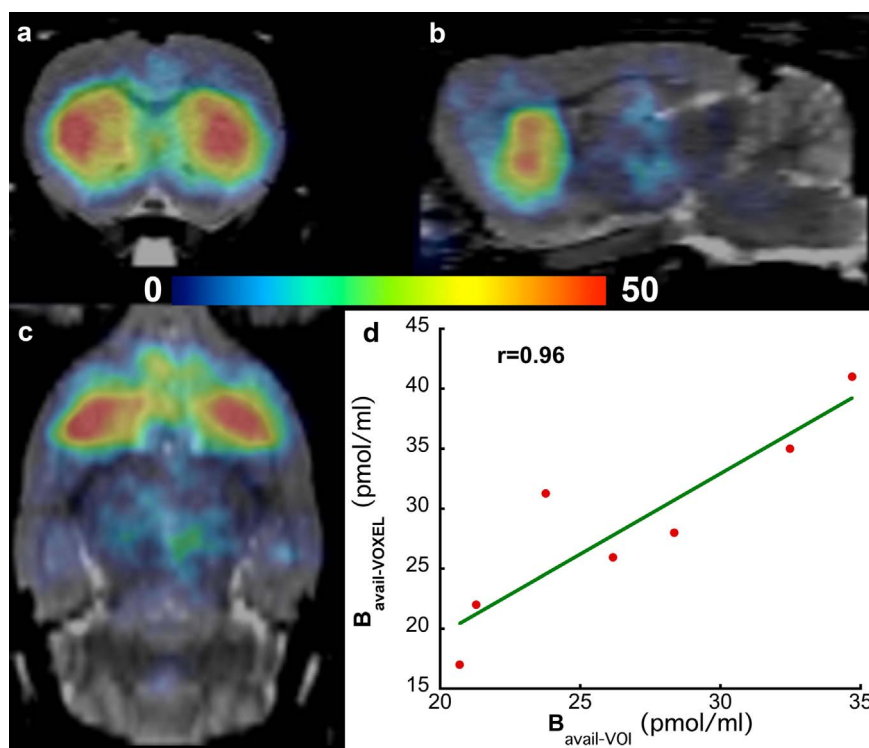


Fig. 5. (a) Coronal, (b) sagittal and (c) axial planes of a parametric B_{avail} images (the image presented here is the average image of 6 rats that underwent the partial saturation protocol and is filtered with a Gaussian kernel with a FWHM of $0.6 \times 0.6 \times 0.6 \text{ mm}^3$). (d) After extraction of the average B_{avail} values in each of the four sub-striatal VOIs, they were compared to the VOI-wise estimated B_{avail} values by means of linear regressions.

and simplifications may need to be applied: a fundamental assumption is that the kinetics of the unlabeled ligand are identical to this of the labeled one (Delforge et al., 1990). Fixing k_{off} to reduce uncertainty in parameter estimations is also necessary for this radiotracer, which, nevertheless, as described elsewhere, does not induce bias in B_{avail} or $appK_d$ estimates (Millet et al., 1995). Measuring the arterial plasma input function also is an invasive and technically difficult procedure, especially in small-animal SPECT and an overestimation of K_1 values may occur, as is the case in the present study (this does not influence B_{avail} and $appK_d$ values, as discussed elsewhere (Dumas et al., 2015)). Despite criticism, the interest of accurately estimating B_{avail} and $appK_d$ is well accepted (Morris et al., 1999). In this context, the partial saturation method is much more interesting for routine research

application given its simplicity and robustness, especially for voxel-wise estimations, as discussed in Section 4.3, especially compared to the multi-injection protocol.

Using cerebellum as reference region for the estimation of BP_{ND} with all three methods (SRTM, LNIGA and SUR) gave excellent correlations with B_{avail} values estimated from full kinetic modeling, the “gold-standard” of kinetic parameters in molecular neuroimaging, thus validating the use of these non-invasive methods. Despite other studies having employed non-invasive approaches before and mainly the SUR with inconsistent time-windows (Crunelle et al., 2012; Meyer et al., 2008a, b, c; Nikolaus et al., 2011; Scherfler et al., 2005; Verhoeff et al., 1991), the present is the only one validating these results against B_{avail} . SRTM and LNIGA applied on scans as short as 70-min long and

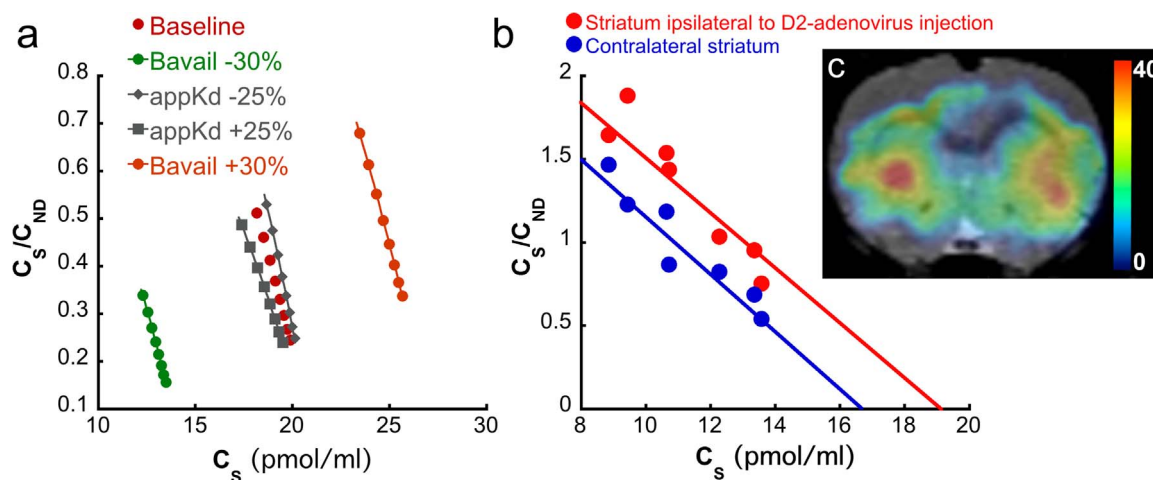


Fig. 6. (a) Scatchard plots corresponding to simulated specific and non-displaceable binding from striatum. Note that the Scatchard equilibrium condition is satisfied in all simulated variations of B_{avail} and $appK_d$, permitting accurate estimation of these parameters. (b) Scatchard plots from a partial saturation experiment in the rat that participated in the adenovirus-mediated D₂-receptor overexpression experiment. Red points correspond to the left striatum, ipsilateral to adenovirus injection, while the blue points correspond to the contralateral striatum. Note the augmentation of B_{avail} whilst $appK_d$ remains virtually stable. (c) Parametric image of B_{avail} (pmol/ml), the injection point is on the left side of the image.

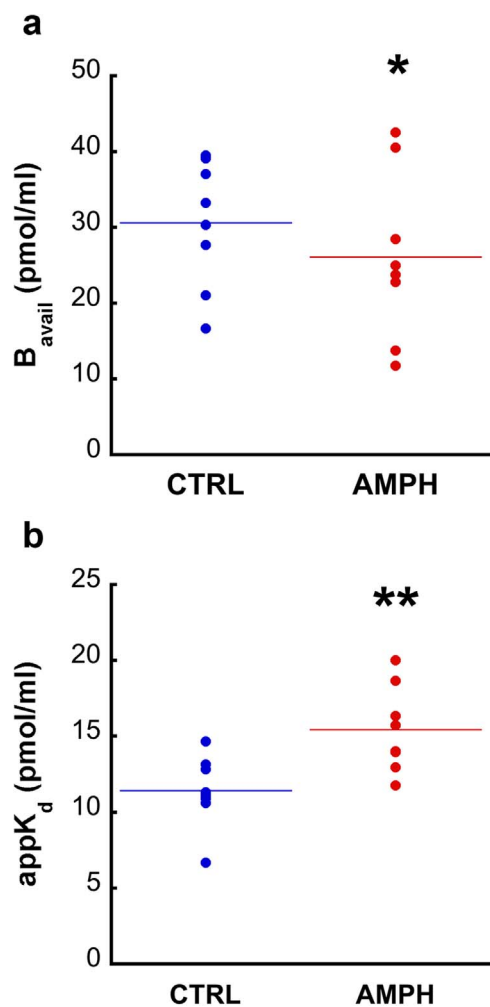


Fig. 7. (a) B_{avail} and (b) $appK_d$ of partial saturation experiments in all four sub-striatal VOIs in two rats. CTRL (in blue color) describes baseline values and AMPH (red), the corresponding values from a second partial saturation study in the same rats, two days after the first and 30 min post-amphetamine administration. Statistically significant differences in B_{avail} and $appK_d$ values after the amphetamine challenge are marked (*, $p < 0.05$ and **, $p < 0.01$).

the SUR, estimated at 80–110 min post radiotracer injection, accurately reflect B_{avail} in rat imaging.

4.2. Impact of non-specific binding on BP_{ND}

An apparent bias in the absolute values of BP_{ND} , when compared to BP values of the 3T-7k likely originates from the difference in non-displaceable binding between striatum and cerebellum. In addition, BP values obtained from the 3T-7k model are quite homogenous across the four striatal subregions, an observation that differs from BP_{ND} values. BP_{ND} values present a difference between CP and NAcc, the latter having consistently lower BP_{ND} . The kinetic pattern of non-specific binding was identified in the multi-injection data using the 3T-7k model (Fig. 1). Non-specific binding is more important in late time-points, in terms of proportion of the total tissue-radioactivity. Thus, the impact of this difference between striatum and cerebellum is only observable in late time-points. This may be clearly observed in the quality of SRTM fits in striatum as a function of the duration of SPECT acquisition: the SRTM fits are excellent and BP_{ND} values are stable when applied on data corresponding to 70–120 min of acquisition. For a scan-duration of more than 120 min, the SRTM model fails to fit the natural decrease in radioactivity in striatum (Fig. 3). To confirm that this misfit derives from the difference in non-specific binding between

striatum and cerebellum, we fitted the data with reference tissue models other than the SRTM, that do not depend on the assumption that the target and reference region present a one tissue-compartment kinetics: the Full-RTM includes a two tissue-compartment model in the target region and a one tissue-compartment in the reference region. Thus, if the misfit were due to the striatal kinetics, Full-RTM would correct it, which is clearly not the case. On the other hand, the 2-TRM, which assumes a two tissue-compartment model kinetics in the reference region, perfectly fits the data for the whole duration of the scan and gives BP_{ND} values that are virtually identical to SRTM-derived values extracted from TACs shorter than 120-min long. As the presence of a specific binding in the cerebellum is excluded by the multi-injection, the second compartment in the cerebellum may conclusively be considered as non-specific binding and the misfit in striatum with SRTM on data longer than 120 min are most probably due to the non-negligible difference in non-specific binding between this region and the cerebellum.

This difference in non-displaceable binding between striatum and cerebellum and within the striatal subregions does not impede the use of these simplified methods, provided that it is stable across different subjects of a given population and independent of the experimental conditions of a biological study. Indeed, the striatal-to-cerebellar non-displaceable distribution volumes (V_{ND}) ratios (1.55 ± 0.08) present a minimal variability, thus supporting this argument for [123 I]IBZM. The excellent correlation of BP_{ND} values with B_{avail} further confirms that BP_{ND} values reflect the absolute receptor concentration. Simplified quantification models generally provide robust kinetic parameters with a lower variability than invasive models that use the plasma-derived input function (Lyoo et al., 2015; Tsartsalis et al., 2016b). BP_{ND} values obtained with the SRTM, LNIGA and SUR present a reasonable variability and may thus be employed as an index of $D_{2/3}$ receptor expression in preclinical biological studies.

4.3. Non-invasive estimation of B_{avail} and $appK_d$ using a partial saturation experiment

A simple method for the estimation of both parameters would be of great interest in the context of translational and clinical molecular imaging. To date, only few biological studies have considered both parameters because their separate estimation is very complicated. This is frequently cited as a limitation of imaging studies of brain physiology and pathology. For instance, regarding normal brain function, Wooten et al. (2012, 2013), after having showed a lack of correlation between B_{avail} and BP_{ND} for the 5-HT_{1A} PET radiotracer [18 F]mefway (Wooten et al., 2012), demonstrated that sex-based differences in BP_{ND} in rhesus monkeys, that could have otherwise been attributed to differences in 5-HT_{1A} receptor concentration (B_{avail}), were actually due to differences in $appK_d$ (Wooten et al., 2013), probably reflecting the endogenous serotonin level. Modifications both in the absolute receptor concentration and endogenous neurotransmitter levels are probably implicated in addiction (Hillmer et al., 2014; Martinez et al., 2012; Wang et al., 1997). Similarly, Vivash et al. (2014) demonstrated that both [18 F]flumazenil-measured GABA_A receptor density and affinity are diminished in epileptic rats. In this case, a reduced $appK_d$ could be attributed, according to the authors, to differences in endogenous ligand concentration (GABA) or into a modified composition of GABA_A receptor subunits. In other words, if $appK_d$ can be robustly dissociated from B_{avail} , valuable information is extracted, which is otherwise only subject to speculation when only BP is estimated. A robust $appK_d$ measurement may permit a more direct study of endogenous ligand level and the detection of more subtle variations across the spectrum of normal and pathological brain function. This is probably not the case in the way the study of endogenous neurotransmitter level is actually performed, that is by evaluating the impact of pharmacologically induced ligand release (e.g. using amphetamine in the case of dopamine) on BP_{ND} . Interestingly, a recent study associated person-

ality traits with endogenous serotonin levels as reflected on 5-HT₄ receptor BP_{ND} (da Cunha-Bang et al., 2016). In this type of studies, using the partial saturation protocol described here could potentially significantly enhance precision when simultaneously estimating serotonin levels (using appK_d) and B_{avail} that is clearly a confounding parameter in BP_{ND} because it may as well vary according to study conditions.

In this paper, we present and validate such a simplified method that employs a partial saturation protocol. This method has been developed by Delforge et al., for the estimation of B_{avail} and appK_d of [¹¹C] flumazenil (Delforge et al., 1996, 1997) and has been employed in clinical research ever since (Bouvard et al., 2005; Freeman et al., 2015). It requires no blood sampling as it relies on cerebellar kinetics for the estimation of the non-displaceable radioactivity fraction in the striatum. Another advantage is that Scatchard equilibrium is rapidly established after injection of a partially saturating dose of unlabeled radiotracer with the radiolabeled one, thus requiring only short scans of a maximum duration of less than 60 min. A preliminary *ex vivo* study demonstrated that a dose between 12 and 24 nmol/kg of unlabeled IBZM, when injected with labeled radiotracer, occupies between 50 and 70% of striatal D_{2/3} receptors. We chose to use the lowest concentration of the spectrum (i.e. 12 nmol/kg) because we considered that saturation of a higher percentage of receptors would lead to very few data-points in the Scatchard equilibrium, given that [¹²³I]IBZM has already a rapid kinetic behavior. Such a dose of unlabeled IBZM induces a rapid decrease in specific binding (Fig. 4a) for a sufficient period of time in order to trace the Scatchard plot.

The results of the partial saturation experiments are in accordance with the B_{avail} and appK_d values obtained with the 3T-7k model on the multi-injection data. B_{avail} values in CP present an apparent over-estimation compared to the respective values from the 3T-7k on multi-injection data. Applying the partial saturation method is based on the assumption that the free binding in the region of interest is described by the kinetics of radioactivity in the reference region after proper correction (Delforge et al., 1996; Wimberley et al., 2014b). As with all simplified methods that use the kinetics in a reference region as an input to the pharmacokinetic model (Slifstein et al., 2000), such a bias in the absolute values is acceptable, as for all other simplified methods of quantification. Regarding the estimation of the r factor that scales the TAC from the cerebellum to better represent the striatal non-displaceable binding, two approaches were employed: in the first one the r value was estimated by the ratio of the V_{ND} values between the striatum and cerebellum (in this case r=1.55), as estimated with the multi-injection approach. The ratio of V_{ND} is in fact not identical to the actual ratio of the C_{ND} in the striatum to the C_{ND} in cerebellum, which is not even perfectly stable during the scan. However, in equilibrium and even in a pseudo-equilibrium condition (that is approached by the Scatchard equilibrium during the partial saturation scan) the ratio of V_{ND} is the best approximation of the striatal-to-cerebellar C_{ND}. The second method that we employed, a presaturation study (Wimberley et al., 2014b) gave an average r value (r=1.68) very close to those estimated with the first method. As discussed by Delforge et al., the presaturation experiment may lead to biased estimates of the non-displaceable binding kinetics (Delforge et al., 1996, 1993) given the fact that the totality of specific binding sites is occupied by the unlabeled ligand, whereas in the partial saturation experiment the occupation is between 50% and 70%. In any case, the simulation study (Supplementary Figure S2) demonstrates that 1) as with all simplified “reference-tissue” methods (Salinas et al., 2015), a difference in the non-displaceable binding leads to biases in the binding parameter values (in this case mainly in B_{avail}) and 2) this bias is virtually identical for a range of simulated B_{avail} values meaning that an existing difference in B_{avail} or appK_d will still be detected regardless of this bias.

To demonstrate the feasibility of performing biological studies of the dopaminergic system with [¹²³I]IBZM with this partial saturation protocol we first performed a simulation study. 30% variations in B_{avail}

and appK_d that are comparable, if not superior, to any biological variation expected in the context of a molecular imaging study were simulated. As the objective of the simulation study was to verify the validity of the Scatchard equilibrium condition, free ligand kinetics was directly extracted from the striatum and not from cerebellum. The results of a partial saturation experiment, considering a fixed dose of unlabeled compound (12 nmol/kg), demonstrated that virtually no bias is introduced in B_{avail} or appK_d. The only considerable parameter that changed in this study was the duration of the Scatchard equilibrium condition. The number of time points that form the Scatchard plot is diminished for lower B_{avail} values.

As a preliminary evaluation of the sensitivity of the partial saturation approach, we induced a unilateral overexpression of D₂ receptors in the striatum of one rat. This permitted a direct comparison of the Scatchard plots from the two regions (shown in Fig. 6b). D₂-receptor overexpression induced an increase in B_{avail} of about 18%, while appK_d remained stable. This finding seems justifiable, as the overexpression of the receptor should increase its concentration. Of course, this experiment is a mere demonstration of the sensitivity of the partial saturation approach. A statistical analysis in a sufficiently large groups of rats should examine the changes in B_{avail} and appK_d after adenovirus injection, to answer in two important questions: 1) whether an overexpression of the receptor actually translates into an increase in the receptor concentration in the brain (so this increase in B_{avail} found here may be confirmed) and 2) whether the increase in receptor concentration follows the cellular and sub-cellular distribution of the receptor at baseline conditions. In this case, no modification of appK_d should be detected (Laruelle, 2000).

Next, we evaluated the feasibility of studying amphetamine-induced dopamine release in striatal sub-regions. This paradigm is widely employed to assess the function of presynaptic dopaminergic terminals (Ginovart, 2005; Laruelle, 2000). Dopamine is thought to act on [¹²³I] IBZM binding by direct competitive antagonistic binding to the D_{2/3} receptor (thereby augmenting the appK_d) as well as by provoking receptors' endocytosis, thereby diminishing receptor concentration that is available for binding (Ginovart et al., 2004; Jongen et al., 2008; Skinbjerg et al., 2010; Sun et al., 2003). Given the complexity of this phenomenon and the potential biological implications, the partial saturation protocol could provide a simple method to assess the impact of the amphetamine challenge on both B_{avail} and appK_d. Our results demonstrate that the partial saturation study is robust enough to detect such changes even at the sub-striatal level. Moreover, they are in accordance with previously reported effects of amphetamine on [¹¹C] raclopride *in vivo* binding in cats, where a 28% decrease in B_{avail} and a 36% increase in appK_d were found (Ginovart et al., 2004). The partial saturation approach permits perhaps a more efficient study of this phenomenon, especially in the light of the results of microdialysis studies that have assessed the kinetics of amphetamine-induced dopamine release (using equivalent administration schemes). Indeed, dopamine concentrations peak rapidly (> 1000-fold) after amphetamine administration and return to baseline, very rapidly at early and more slowly at late time-points (Breier et al., 1997; Butcher et al., 1988; Kuczenski and Segal, 1989; Laruelle et al., 1997; Shoblock et al., 2003; Tsukada et al., 1999). The time-window in which our experiments are performed (that is roughly at 40–75 min after amphetamine administration) falls within a period during which dopamine concentrations decrease relatively slowly and are certainly still significantly higher than baseline. Based on current literature and quantification methods, the partial saturation method seems to be one of the most appropriate for this purpose, at least in terms of simplicity and timing. Previous studies of this phenomenon that dissociated B_{avail} from appK_d estimates have employed complex and long scan protocols composed of three or four scans overall (because of the need to perform scans with different specific activities) with a total duration well beyond the temporal window in which the dopamine release can be captured (Ginovart et al., 2004) while an important effect of timing of scans after

induction of dopamine release has been demonstrated (Doudet and Holden, 2003a, b; Doudet et al., 2003; Doudet et al., 2006).

The partial saturation method in [123 I]IBZM imaging has potential applications in clinical SPECT imaging. The arguments exposed in previous paragraphs, in favor of the separate study of B_{avail} and appK_d are even more prominent in clinical imaging studies of the dopaminergic system. The complexity of the human brain may not be diminished to the study of animal models that only approach some of the aspects of brain physiology and disease while others remain totally out of reach (to cite only few of them; higher cognitive processes and pathological conditions such as perception and thought disorders). In addition, brain neurochemistry underlies a plexus of functional and pathological properties that compose the clinical picture: for instance, psychiatric pathologies are often present in several dimensions going from acute “diseases” to permanent traits of personality that potentially interact with both the quantity of a neurotransmitter receptor and the endogenous neurotransmitter concentration that may not be assessed with the BP. That said, the development of clinical molecular imaging has been a capital step towards a better understanding of how the brain functions and dysfunctions. The possibility for a more in-depth study with the partial saturation protocol, which is as technically feasible as currently employed methods to estimate BP_{ND} is highly promising to alleviate the confounding effect of appK_d on B_{avail} and vice versa. To date, variations BP may not be conclusively attributed to differences in actual receptor concentration or in endogenous dopamine quantity and this confounding effect (to cite only a few relevant studies; (Egerton et al., 2009; Howes et al., 2009, 2012; Tomasi et al., 2016; Vaessen et al., 2015; Volkow et al., 2007, 2009b, 2008; Wiers et al., 2016)) is only approached theoretically. Assessing appK_d may also permit the (indirect) evaluation of the level of endogenous dopamine without relying on the stimulant-induced dopamine release paradigm that not only involves the administration of the stimulant agent but also presents an important biological complexity *per se* (Laruelle, 2000). Currently employed methods to separately estimate B_{avail} and appK_d are very difficult to employ in routine clinical research and are practically limited to animal and very rarely in human studies (Delforge et al., 1993; Doudet et al., 2003; Ginovart et al., 2004; Millet et al., 2000a, 2006). Regarding the feasibility of applying the partial saturation protocol in clinical [123 I]IBZM SPECT, it should not be problematic, in theory. Indeed, occupying 50–70% of striatal $D_{2/3}$ receptors for the application of the partial saturation approach induces little, if any, adverse effects. Indeed, this level of blockade is identical to the one induced by antipsychotic agents at therapeutic doses and it is accepted that adverse events appear when blockade is higher than 80–85% (Ginovart and Kapur, 2012). Proper validation of safety of administering partially saturating doses of unlabeled IBZM through animal and clinical studies could thus permit the application of this protocol in clinical imaging where its impact in the understanding of brain function and disease would be invaluable.

4.4. Denoising of [123 I]IBZM SPECT images with FA

SPECT images are particularly noised. Employing raw images for analysis was in fact particularly difficult, even when TACs extracted from the whole-striatal VOI were considered. Indeed, the variability of 3T-7k-derived parameters from the multi-injection study was high in raw images (data not shown). In the case of partial saturation scans, noise induced important deviations from linearity in Scatchard plots and a high uncertainty in estimations as linear fits were of poor quality (data not shown). We thus employed FA, as previously described (Di Paola et al., 1982; Millet et al., 2012; Tsartsalis et al., 2016a), retaining four prevalent factors that efficiently removes noise while inducing negligible bias (if any), given that is a relatively “conservative” configuration, compared to a two- (Tsartsalis et al., 2016a) or three-factor analysis applied before (Tsartsalis et al., 2014). FA notably permits to construct valid parametric images of B_{avail} using the partial

saturation method, as demonstrated by the quality of parametric images and the excellent correlation of the voxel-wise estimated results with their VOI-estimated counterparts. It is important to note that FA application may also correct for the contamination of brain structures under study with radioactivity from adjacent structures due to partial volume effects (Millet et al., 2012).

5. Conclusion

In conclusion, we validate here the use of simplified methods for the estimation of either BP_{ND} or B_{avail} and appK_d . SRTM and LNIGA applied on 70-minute long scans and SUR applied on data corresponding to a static scan between 80 and 110 minutes after radiotracer injection may robustly provide BP_{ND} estimates that accurately reflect the B_{avail} estimation after full kinetic modeling of [123 I]IBZM. We also describe here a simplified and robust method for the separate estimation of B_{avail} and appK_d , at both the VOI- and the voxel-level for a more in-depth study of the absolute receptor quantity in striatum and the interactions between receptor and endogenous ligand. This method may thus be used for more technically demanding studies of the dopaminergic system, such as the amphetamine-induced dopamine release effect in translational and, potentially, in clinical imaging studies.

Acknowledgements

This work was supported by the Swiss National Science Foundation (grant no. 310030_156829), by the Geneva Neuroscience Center and by the Maria Zausi Memorial Foundation (Greece) through a scholarship of the Hellenic State Scholarship Foundation (ST) and by the “Swiss Association for Alzheimer's Research” which was created in 2009 to finance Swiss fundamental and clinical research programs on Alzheimer's disease. Authors are grateful to Mrs Maria Surini-Demiri for excellent technical assistance and declare that they have no conflict of interest.

Appendix A. Supplementary material

Supplementary data associated with this article can be found in the online version at <http://dx.doi.org/10.1016/j.neuroimage.2016.12.050>.

References

- Abi-Dargham, A., van de Giessen, E., Slifstein, M., Kegeles, L.S., Laruelle, M., 2009. Baseline and amphetamine-stimulated dopamine activity are related in drug-naïve schizophrenic subjects. *Biol. Psychiatry* 65, 1091–1093.
- Bouvard, S., Costes, N., Bonnefoi, F., Lavenne, F., Mauguier, F., Delforge, J., Ryvlin, P., 2005. Seizure-related short-term plasticity of benzodiazepine receptors in partial epilepsy: a [^{11}C]flumazenil-PET study. *Brain* 128, 1330–1343.
- Breier, A., Su, T.P., Saunders, R., Carson, R.E., Kolachana, B.S., de Bartolomeis, A., Weinberger, D.R., Weisenfeld, N., Malhotra, A.K., Eckelman, W.C., Pickar, D., 1997. Schizophrenia is associated with elevated amphetamine-induced synaptic dopamine concentrations: evidence from a novel positron emission tomography method. *Proc. Natl. Acad. Sci. USA* 94, 2569–2574.
- Butcher, S.P., Fairbrother, I.S., Kelly, J.S., Arbuthnott, G.W., 1988. Amphetamine-induced dopamine release in the rat striatum: an in vivo microdialysis study. *J. Neurochem.* 50, 346–355.
- Crunelle, C.L., de Wit, T.C., de Bruin, K., Ramakers, R.M., van der Have, F., Beekman, F.J., van den Brink, W., Booij, J., 2012. Varenicline increases in vivo striatal dopamine $D(2/3)$ receptor binding: an ultra-high-resolution pinhole [^{123}I]IBZM SPECT study in rats. *Nucl. Med. Biol.*
- da Cunha-Bang, S., Mc Mahon, B., MacDonald Fisher, P., Jensen, P.S., Svarer, C., Moos Knudsen, G., 2016. High trait aggression in men is associated with low 5-HT levels, as indexed by 5-HT $_4$ receptor binding. *Soc. Cogn. Affect. Neurosci.* 11, 548–555.
- Delforge, J., Bottlaender, M., Loc'h, C., Guenther, I., Fuseau, C., Bendriem, B., Syrota, A., Maziere, B., 1999. Quantitation of extrastriatal D2 receptors using a very high-affinity ligand (FLB 457) and the multi-injection approach. *J. Cereb. Blood Flow. Metab.* 19, 533–546.
- Delforge, J., Spelle, L., Bendriem, B., Samson, Y., Bottlaender, M., Papageorgiou, S., Syrota, A., 1996. Quantitation of benzodiazepine receptors in human brain using the partial saturation method. *J. Nucl. Med.* 37, 5–11.

- Delforge, J., Spelle, L., Bendriem, B., Samson, Y., Syrota, A., 1997. Parametric images of benzodiazepine receptor concentration using a partial-saturation injection. *J. Cereb. Blood Flow. Metab.* 17, 343–355.
- Delforge, J., Syrota, A., Bottlaender, M., Varastet, M., Loc'h, C., Bendriem, B., Crouzel, C., Brouillet, E., Maziere, M., 1993. Modeling analysis of [¹¹C]flumazenil kinetics studied by PET: application to a critical study of the equilibrium approaches. *J. Cereb. Blood Flow. Metab.* 13, 454–468.
- Delforge, J., Syrota, A., Mazoyer, B.M., 1989. Experimental design optimisation: theory and application to estimation of receptor model parameters using dynamic positron emission tomography. *Phys. Med. Biol.* 34, 419–435.
- Delforge, J., Syrota, A., Mazoyer, B.M., 1990. Identifiability analysis and parameter identification of an in vivo ligand-receptor model from PET data. *IEEE Trans. Biomed. Eng.* 37, 653–661.
- Di Paola, R., Bazin, J.P., Aubry, F., Aurengo, A., Cavaillols, F., Herry, J.Y., Kahn, E., 1982. Handling of dynamic sequences in nuclear medicine. *IEEE Trans. Nucl. Sci.* NS29, 1310–1321.
- Doudet, D.J., Holden, J.E., 2003a. Raclopride studies of dopamine release: dependence on presynaptic integrity. *Biol. Psychiatry* 54, 1193–1199.
- Doudet, D.J., Holden, J.E., 2003b. Sequential versus nonsequential measurement of density and affinity of dopamine D2 receptors with [¹¹C]raclopride: effect of methamphetamine. *J. Cereb. Blood Flow. Metab.* 23, 1489–1494.
- Doudet, D.J., Jivan, S., Holden, J.E., 2003. In vivo measurement of receptor density and affinity: comparison of the routine sequential method with a nonsequential method in studies of dopamine D2 receptors with [¹¹C]raclopride. *J. Cereb. Blood Flow. Metab.* 23, 280–284.
- Doudet, D.J., Ruth, T.J., Holden, J.E., 2006. Sequential versus nonsequential measurement of density and affinity of dopamine D2 receptors with [¹¹C]raclopride: 2: effects of DAT inhibitors. *J. Cereb. Blood Flow. Metab.* 26, 28–37.
- Dumas, N., Moulin-Sallanon, M., Fender, P., Tournier, B.B., Ginovart, N., Charnay, Y., Millet, P., 2015. In Vivo Quantification of 5-HT_{2A} Brain Receptors in Mdr1a KO Rats with 123I-R91150 Single-Photon Emission Computed Tomography. *Mol. Imaging*, 14.
- Egerton, A., Mehta, M.A., Montgomery, A.J., Lappin, J.M., Howes, O.D., Reeves, S.J., Cunningham, V.J., Grasby, P.M., 2009. The dopaminergic basis of human behaviors: a review of molecular imaging studies. *Neurosci. Biobehav. Rev.* 33, 1109–1132.
- Freeman, L., Garcia-Lorenzo, D., Bottin, L., Leroy, C., Louapre, C., Bodini, B., Papeix, C., Assouad, R., Granger, B., Tourbah, A., Dolle, F., Lubetzki, C., Bottlaender, M., Stankoff, B., 2015. The neuronal component of gray matter damage in multiple sclerosis: a [(11)C]flumazenil positron emission tomography study. *Ann. Neurol.* 78, 554–567.
- Gandelman, M.S., Baldwin, R.M., Zoghbi, S.S., Zea-Ponce, Y., Innis, R.B., 1994. Evaluation of ultrafiltration for the free-fraction determination of single photon emission computed tomography (SPECT) radiotracers: beta-cit, IBF, and iomazenil. *J. Pharm. Sci.* 83, 1014–1019.
- Ginovart, N., 2005. Imaging the dopamine system with in vivo [¹¹C]raclopride displacement studies: understanding the true mechanism. *Mol. Imaging Biol.* 7, 45–52.
- Ginovart, N., Kapur, S., 2012. Role of dopamine D(2) receptors for antipsychotic activity. *Handb. Exp. Pharmacol.*, 27–52.
- Ginovart, N., Wilson, A.A., Houle, S., Kapur, S., 2004. Amphetamine pretreatment induces a change in both D2-Receptor density and apparent affinity: a [¹¹C]raclopride positron emission tomography study in cats. *Biol. Psychiatry* 55, 1188–1194.
- Ginovart, N., Wilson, A.A., Meyer, J.H., Hussey, D., Houle, S., 2001. Positron emission tomography quantification of [(11)C]-DASB binding to the human serotonin transporter: modeling strategies. *J. Cereb. Blood Flow. Metab.* 21, 1342–1353.
- Gunn, R.N., Lammertsma, A.A., Hume, S.P., Cunningham, V.J., 1997. Parametric imaging of ligand-receptor binding in PET using a simplified reference region model. *Neuroimage* 6, 279–287.
- Hillmer, A.T., Wooten, D.W., Tudorascu, D.L., Barnhart, T.E., Ahlers, E.O., Resch, L.M., Larson, J.A., Converse, A.K., Moore, C.F., Schneider, M.L., Christian, B.T., 2014. The effects of chronic alcohol self-administration on serotonin-1A receptor binding in nonhuman primates. *Drug Alcohol Depend.* 144, 119–126.
- Howes, O.D., Egerton, A., Allan, V., McGuire, P., Stokes, P., Kapur, S., 2009. Mechanisms underlying psychosis and antipsychotic treatment response in schizophrenia: insights from PET and SPECT imaging. *Curr. Pharm. Des.* 15, 2550–2559.
- Howes, O.D., Kambeitz, J., Kim, E., Stahl, D., Slifstein, M., Abi-Dargham, A., Kapur, S., 2012. The nature of dopamine dysfunction in schizophrenia and what this means for treatment. *Arch. Gen. Psychiatry* 69, 776–786.
- Innis, R.B., Cunningham, V.J., Delforge, J., Fujita, M., Gjedde, A., Gunn, R.N., Holden, J., Houle, S., Huang, S.C., Ichise, M., Iida, H., Ito, H., Kimura, Y., Koeppe, R.A., Knudsen, G.M., Knuuti, J., Lammertsma, A.A., Laruelle, M., Logan, J., Maguire, R.P., Mintun, M.A., Morris, E.D., Parsey, R., Price, J.C., Slifstein, M., Sossi, V., Suhara, T., Votaw, J.R., Wong, D.F., Carson, R.E., 2007. Consensus nomenclature for in vivo imaging of reversibly binding radioligands. *J. Cereb. Blood Flow. Metab.* 27, 1533–1539.
- Jongen, C., de Bruin, K., Beekman, F., Booij, J., 2008. SPECT imaging of D2 dopamine receptors and endogenous dopamine release in mice. *Eur. J. Nucl. Med. Mol. Imaging* 35, 1692–1698.
- Kuczenski, R., Segal, D., 1989. Concomitant characterization of behavioral and striatal neurotransmitter response to amphetamine using in vivo microdialysis. *J. Neurosci.* 9, 2051–2065.
- Kugaya, A., Fujita, M., Innis, R.B., 2000. Applications of SPECT imaging of dopaminergic neurotransmission in neuropsychiatric disorders. *Ann. Nucl. Med.* 14, 1–9.
- Kuwabara, H., McCaul, M.E., Wand, G.S., Earley, C.J., Allen, R.P., Weerts, E.M., Dannals, R.F., Wong, D.F., 2012. Dissociative changes in the Bmax and KD of dopamine D2/D3 receptors with aging observed in functional subdivisions of the striatum: a revisit with an improved data analysis method. *J. Nucl. Med.* 53, 805–812.
- Lammertsma, A.A., Bench, C.J., Hume, S.P., Osman, S., Gunn, K., Brooks, D.J., Frackowiak, R.S., 1996. Comparison of methods for analysis of clinical [¹¹C]raclopride studies. *J. Cereb. Blood Flow. Metab.* 16, 42–52.
- Lammertsma, A.A., Hume, S.P., 1996. Simplified reference tissue model for PET receptor studies. *Neuroimage* 4, 153–158.
- Laruelle, M., 2000. Imaging synaptic neurotransmission with in vivo binding competition techniques: a critical review. *J. Cereb. Blood Flow. Metab.* 20, 423–451.
- Laruelle, M., Iyer, R.N., al-Tikriti, M.S., Zea-Ponce, Y., Malison, R., Zoghbi, S.S., Baldwin, R.M., Kung, H.F., Charney, D.S., Hoffer, P.B., Innis, R.B., Bradberry, C.W., 1997. Microdialysis and SPECT measurements of amphetamine-induced dopamine release in nonhuman primates. *Synapse* 25, 1–14.
- Logan, J., Fowler, J.S., Volkow, N.D., Wang, G.J., Ding, Y.S., Alexoff, D.L., 1996. Distribution volume ratios without blood sampling from graphical analysis of PET data. *J. Cereb. Blood Flow. Metab.* 16, 834–840.
- Lyoo, C.H., Ikawa, M., Liow, J.S., Zoghbi, S.S., Morse, C.L., Pike, V.W., Fujita, M., Innis, R.B., Kreisl, W.C., 2015. Cerebellum Can Serve As a Pseudo-Reference Region in Alzheimer Disease to Detect Neuroinflammation Measured with PET Radioligand Binding to Translocator Protein. *J. Nucl. Med.* 56, 701–706.
- Martinez, D., Saccone, P.A., Liu, F., Slifstein, M., Orlovsky, D., Grassetti, A., Cook, S., Broft, A., Van Heertum, R., Comer, S.D., 2012. Deficits in dopamine D(2) receptors and presynaptic dopamine in heroin dependence: commonalities and differences with other types of addiction. *Biol. Psychiatry* 71, 192–198.
- Mauger, G., Saba, W., Hantraye, P., Dolle, F., Coulon, C., Bramoulle, Y., Chalon, S., Gregoire, M.C., 2005. Multiinjection approach for D2 receptor binding quantification in living rats using [¹¹C]raclopride and the beta-microprobe: crossvalidation with in vitro binding data. *J. Cereb. Blood Flow. Metab.* 25, 1517–1527.
- Meyer, P.T., Salber, D., Schiefer, J., Cremer, M., Schaefer, W.M., Kosinski, C.M., Langen, K.J., 2008a. Cerebral kinetics of the dopamine D(2) receptor ligand [(123)I]IBZM in mice. *Nucl. Med. Biol.* 35, 467–473.
- Meyer, P.T., Salber, D., Schiefer, J., Cremer, M., Schaefer, W.M., Kosinski, C.M., Langen, K.J., 2008b. Comparison of intravenous and intraperitoneal [(123)I]IBZM injection for dopamine D2 receptor imaging in mice. *Nucl. Med. Biol.* 35, 543–548.
- Meyer, P.T., Sattler, B., Winz, O.H., Fundke, R., Oehlwein, C., Kendziorra, K., Hesse, S., Schaefer, W.M., Sabri, O., 2008c. Kinetic analyses of [(123)I]IBZM SPECT for quantification of striatal dopamine D2 receptor binding: a critical evaluation of the single-scan approach. *Neuroimage* 42, 548–558.
- Millet, P., Delforge, J., Mauguire, F., Pappata, S., Cinotti, L., Frouin, V., Samson, Y., Bendriem, B., Syrota, A., 1995. Parameter and index images of benzodiazepine receptor concentration in the brain. *J. Nucl. Med.* 36, 1462–1471.
- Millet, P., Graf, C., Buck, A., Walder, B., Ibanez, V., 2002. Evaluation of the reference tissue models for PET and SPECT benzodiazepine binding parameters. *Neuroimage* 17, 928–942.
- Millet, P., Graf, C., Buck, A., Walder, B., Westera, G., Broggin, C., Arigoni, M., Slosman, D., Bouras, C., Ibanez, V., 2000a. Similarity and robustness of PET and SPECT binding parameters for benzodiazepine receptors. *J. Cereb. Blood Flow. Metab.* 20, 1587–1603.
- Millet, P., Graf, C., Moulin, M., Ibanez, V., 2006. SPECT quantification of benzodiazepine receptor concentration using a dual-ligand approach. *J. Nucl. Med.* 47, 783–792.
- Millet, P., Ibanez, V., Delforge, J., Pappata, S., Guimon, J., 2000b. Wavelet analysis of dynamic PET data: application to the parametric imaging of benzodiazepine receptor concentration. *Neuroimage* 11, 458–472.
- Millet, P., Moulin, M., Bartoli, A., Del Guerra, A., Ginovart, N., Lemoucheux, L., Buono, S., Fagret, D., Charnay, Y., Ibanez, V., 2008. In vivo quantification of 5-HT_{1A}-[18F]MPPE interactions in rats using the YAP-(S)PET scanner and a beta-microprobe. *Neuroimage* 41, 823–834.
- Millet, P., Moulin-Sallanon, M., Tournier, B.B., Dumas, N., Charnay, Y., Ibanez, V., Ginovart, N., 2012. Quantification of dopamine D(2/3) receptors in rat brain using factor analysis corrected [18F]fallypride images. *Neuroimage* 62, 1455–1468.
- Mintun, M.A., Raichle, M.E., Kilbourn, M.R., Wooten, G.F., Welch, M.J., 1984. A quantitative model for the in vivo assessment of drug binding sites with positron emission tomography. *Ann. Neurol.* 15, 217–227.
- Morris, E.D., Bonab, A.A., Alpert, N.M., Fischman, A.J., Madras, B.K., Christian, B.T., 1999. Concentration of dopamine transporters: to Bmax or not to Bmax? *Synapse* 32, 136–140.
- Murnane, K.S., Howell, L.L., 2011. Neuroimaging and drug taking in primates. *Psychopharmacol. (Berl.)* 216, 153–171.
- Narendran, R., Martinez, D., 2008. Cocaine abuse and sensitization of striatal dopamine transmission: a critical review of the preclinical and clinical imaging literature. *Synapse* 62, 851–869.
- Nikolaus, S., Antke, C., Beu, M., Kley, K., Wirtwar, A., Huston, J.P., Muller, H.W., 2011. Binding of [(123)I]iodobenzamide to the rat D2 receptor after challenge with various doses of methylphenidate: an in vivo imaging study with dedicated small animal SPECT. *Eur. J. Nucl. Med. Mol. Imaging* 38, 694–701.
- Salinas, C.A., Searle, G.E., Gunn, R.N., 2015. The simplified reference tissue model: model assumption violations and their impact on binding potential. *J. Cereb. Blood Flow. Metab.* 35, 304–311.
- Scherflier, C., Scholz, S.W., Donnemiller, E., Decristoforo, C., Oberladstatter, M., Stefanova, N., Diederer, E., Virgolini, I., Poewe, W., Wenning, G.K., 2005. Evaluation of [(123)I]IBZM pinhole SPECT for the detection of striatal dopamine D2 receptor availability in rats. *Neuroimage* 24, 822–831.
- Schiffer, W.K., Mirrione, M.M., Biegona, A., Alexoff, D.L., Patel, V., Dewey, S.L., 2006. Serial microPET measures of the metabolic reaction to a microdialysis probe implant. *J. Neurosci. Method.* 155, 272–284.

- Shoblock, J.R., Sullivan, E.B., Maisonneuve, I.M., Glick, S.D., 2003. Neurochemical and behavioral differences between d-methamphetamine and d-amphetamine in rats. *Psychopharmacol. (Berl.)* 165, 359–369.
- Shrestha, S., Hirvonen, J., Hines, C.S., Henter, I.D., Svenningsson, P., Pike, V.W., Innis, R.B., 2012. Serotonin-1A receptors in major depression quantified using PET: controversies, confounds, and recommendations. *Neuroimage* 59, 3243–3251.
- Skinbjerg, M., Seneca, N., Liow, J.S., Hong, J., Weinshenker, D., Pike, V.W., Halldin, C., Sibley, D.R., Innis, R.B., 2010. Dopamine beta-hydroxylase-deficient mice have normal densities of D(2) dopamine receptors in the high-affinity state based on in vivo PET imaging and in vitro radioligand binding. *Synapse* 64, 699–703.
- Slifstein, M., Parsey, R.V., Laruelle, M., 2000. Derivation of [(11)C]WAY-100635 binding parameters with reference tissue models: effect of violations of model assumptions. *Nucl. Med. Biol.* 27, 487–492.
- Sun, W., Ginovart, N., Ko, F., Seeman, P., Kapur, S., 2003. In vivo evidence for dopamine-mediated internalization of D2-receptors after amphetamine: differential findings with [3H]raclopride versus [3H]spiperone. *Mol. Pharmacol.* 63, 456–462.
- Tomasi, D., Wang, G.J., Volkow, N.D., 2016. Association between striatal dopamine D2/D3 receptors and brain activation during visual attention: effects of sleep deprivation. *Transl. Psychiatry* 6, e828.
- Tsartsalis, S., Moulin-Sallanon, M., Dumas, N., Tournier, B.B., Ghezzi, C., Charnay, Y., Ginovart, N., Millet, P., 2014. Quantification of GABAA receptors in the rat brain with [(123)I]iomazenil SPECT from factor analysis-denoised images. *Nucl. Med. Biol.* 41, 186–195.
- Tsartsalis, S., Tournier, B.B., Ginovart, N., Ibanez, V., Millet, P., 2016a. Exploring the full potential of factor analysis for the optimization of voxel-wise parameter estimation and inference analysis with Statistical Parametric Mapping in molecular neuroimaging. Submitted.
- Tsartsalis, S., Tournier, B.B., Huynh-Gatz, T., Dumas, N., Ginovart, N., Moulin-Sallanon, M., Millet, P., 2015. 5-HT2A receptor SPECT imaging with [I]R91150 under P-gp inhibition with tariquidar: More is better? *Nucl. Med. Biol.*
- Tsartsalis, S., Tournier, B.B., Huynh-Gatz, T., Dumas, N., Ginovart, N., Moulin-Sallanon, M., Millet, P., 2016b. 5-HT2A receptor SPECT imaging with [(1)(2)(3)I]R91150 under P-gp inhibition with tariquidar: more is better? *Nucl. Med. Biol.* 43, 81–88.
- Tsukada, H., Nishiyama, S., Kakiuchi, T., Ohba, H., Sato, K., Harada, N., 1999. Is synaptic dopamine concentration the exclusive factor which alters the in vivo binding of [(11)C]raclopride? pet studies combined with microdialysis in conscious monkeys. *Brain Res* 841, 160–169.
- Vaessen, T., Hernaus, D., Myin-Germeys, I., van Amelsvoort, T., 2015. The dopaminergic response to acute stress in health and psychopathology: a systematic review. *Neurosci. Biobehav. Rev.* 56, 241–251.
- Verhoeff, N.P., Bobeldijk, M., Feenstra, M.G., Boer, G.J., Maas, M.A., Erdtsieck-Ernste, E., de Bruin, K., van Royen, E.A., 1991. In vitro and in vivo D2-dopamine receptor binding with [(123)I]S(-) iodobenzamide [(123)IBZM] in rat and human brain. *Int. J. Rad. Appl. Instrum. B* 18, 837–846.
- Vivash, L., Gregoire, M.C., Boullieret, V., Berard, A., Wimberley, C., Binns, D., Roselt, P., Katsifis, A., Myers, D.E., Hicks, R.J., O'Brien, T.J., Dedeurwaerdere, S., 2014. In vivo measurement of hippocampal GABAA/cBZR density with [(18)F]-flumazenil PET for the study of disease progression in an animal model of temporal lobe epilepsy. *PLoS One* 9, e86722.
- Volkow, N.D., Fowler, J.S., Wang, G.J., Baler, R., Telang, F., 2009a. Imaging dopamine's role in drug abuse and addiction. *Neuropharmacology* 56 (Suppl 1), 3–8.
- Volkow, N.D., Fowler, J.S., Wang, G.J., Swanson, J.M., Telang, F., 2007. Dopamine in drug abuse and addiction: results of imaging studies and treatment implications. *Arch. Neurol.* 64, 1575–1579.
- Volkow, N.D., Tomasi, D., Wang, G.J., Telang, F., Fowler, J.S., Wang, R.L., Logan, J., Wong, C., Jayne, M., Swanson, J.M., 2009b. Hyperstimulation of striatal D2 receptors with sleep deprivation: implications for cognitive impairment. *Neuroimage* 45, 1232–1240.
- Volkow, N.D., Wang, G.J., Telang, F., Fowler, J.S., Logan, J., Wong, C., Ma, J., Pradhan, K., Tomasi, D., Thanos, P.K., Ferre, S., Jayne, M., 2008. Sleep deprivation decreases binding of [(11)C]raclopride to dopamine D2/D3 receptors in the human brain. *J. Neurosci.* 28, 8454–8461.
- Wang, G.J., Volkow, N.D., Fowler, J.S., Logan, J., Abumrad, N.N., Hitzemann, R.J., Pappas, N.S., Pascani, K., 1997. Dopamine D2 receptor availability in opiate-dependent subjects before and after naloxone-precipitated withdrawal. *Neuropsychopharmacology* 16, 174–182.
- Watabe, H., Carson, R.E., Iida, H., 2000. The reference tissue model: three compartments for the reference region. *Neuroimage*, 11.
- Wiers, C.E., Shumay, E., Cabrera, E., Shokri-Kojori, E., Gladwin, T.E., Skarda, E., Cunningham, S.I., Kim, S.W., Wong, T.C., Tomasi, D., Wang, G.J., Volkow, N.D., 2016. Reduced sleep duration mediates decreases in striatal D2/D3 receptor availability in cocaine abusers. *Transl. Psychiatry* 6, e752.
- Wimberley, C., Angelis, G., Boisson, F., Callaghan, P., Fischer, K., Pichler, B.J., Meikle, S.R., Gregoire, M.C., Reilhac, A., 2014a. Simulation-based optimisation of the PET data processing for Partial Saturation Approach protocols. *Neuroimage* 97c, 29–40.
- Wimberley, C.J., Fischer, K., Reilhac, A., Pichler, B.J., Gregoire, M.C., 2014b. A data driven method for estimation of B and appK using a single injection protocol with [(11)C]raclopride in the mouse. *Neuroimage*.
- Wooten, D.W., Hillmer, A.T., Moirano, J.M., Ahlers, E.O., Slesarev, M., Barnhart, T.E., Mukherjee, J., Schneider, M.L., Christian, B.T., 2012. Measurement of 5-HT(1A) receptor density and in-vivo binding parameters of [(18)F]mefway in the nonhuman primate. *J. Cereb. Blood Flow. Metab.* 32, 1546–1558.
- Wooten, D.W., Hillmer, A.T., Moirano, J.M., Tudorascu, D.L., Ahlers, E.O., Slesarev, M.S., Barnhart, T.E., Mukherjee, J., Schneider, M.L., Christian, B.T., 2013. 5-HT1A sex based differences in Bmax, in vivo KD, and BPND in the nonhuman primate. *Neuroimage* 77, 125–132.